Long-term Associations of Near-coastal Ocean Waves with Microseisms and Storm Surge: 1992-2017

Peter D. Bromirski
Scripps Institution of Oceanography
University of California San Diego,
La Jolla, California, USA

Introduction

The relationship between near-coastal ocean waves and double-frequency (DF) microseism activity has been well established over relatively short time periods, ranging from synoptic to seasonal to annual intervals. While some DF microseism signals undoubtedly arrive from non-local coastal regions (*Bromirski and Duennebier*, 2002; *Bromirski et al*., 2005), and from the deep ocean (*Obrebski et al*., 200X; *Ardhuin et al*., 20XX; *Bromirski et al*., 2013; …), the preponderance of data indicate that the dominant contribution to near-coastal DF microseism levels results from relatively nearby coastal wave activity (*Bromirski et al*., 1999; *Bromirski and Duennebier*, 2002). Here we examine the association of buoy-measured ocean wave activity along the central California coast with a 25-year seismic record at Berkeley, CA to determine the consistency of their long-term variability. To assess the reliability of such comparisons for estimating wave climate variability from DF seismic data, the incidence of anomalous seismic signals relative to nearby buoy wave heights, i.e. high wave heights with low microseism levels and low wave heights with high microseism levels, are investigated. The intent is to determine whether anomalous signals would significantly affect the statistics of wave variability determined from near-coastal microseism variability, with the long-term goal to reconstruct the wave climate (prior to the buoy record) from digitized analog seismic recordings at Berkeley spanning 1931-1981 to assess interdecadal wave climate variability along the central California coast.

Seismic data:

All available digital broadband 1 Hz-sampled vertical component data recorded at the Berkeley, CA seismic station (BKS) spanning the 1992-2017 epoch were downloaded from the Northern California Earthquake Data Center (NCEDC). Spectra, corrected for the instrument response were computed with Welch averaging using 512 s data segments and 256 s FFT length, then stepping 64 s to the next 512 s segment. The overlapping methodology employed yields relatively smooth temporal spectral variability in the DF microseism band. Earthquake and other transient signals were then excluded. Hour averages of the spectral estimates were then obtained, with seismic rms amplitudes, S_{DF}, of the hour-averaged spectra over the [0.085, 0.45] Hz DF microseism band determined.

Buoy Data:

All available hourly significant wave height (Hs) data measured at nearby National Oceanic and Atmospheric Administration (NOAA) buoy 46013 spanning 1992-2017 were downloaded from the National Oceanic Data Center (NODC). These were used to establish the association with S_{DF} levels.

Storm Surge:

All available hourly tide gauge data recorded at the San Francisco Fort Point tide gauge (SFO) were downloaded from the NOAA National Oceanic Service (NOS). The non-tide water level heights were obtained using the spectral filtering methodology presented in *Bromirski et al*. (2003). Anomalous transients were removed, resulting in a smoothly varying non-tide (storm surge) record spanning 1992-2017.

Wave and Associated Seismic and Storm Surge Events:

Wave Hs observations at buoy 46013 do not necessarily occur simultaneously with associated microseism peaks because of: (1) the expanse of the storm wave extent, (2) Hs variability along the coast due to wave refraction due to continental shelf bottom topography that depends on wave approach angle, (3) general propagation direction, i.e. wave fronts propagating nearly north-south will illuminate a smaller coastal region than wave fronts coming from the west, which in turn could result in S_{DF} generated from interactions between incoming and coastally-reflected wave components being in phase and result in higher amplitude S_{DF} than would be anticipated from moderate amplitude Hs, (4) the magnitude of coastally-reflected wave components likely changes with season since beach slopes steepen from progressive wave activity during winter, (5) wave-wave interactions over the North American continental shelf, and (6) DF microseism generation along distant coastlines or far from the coast, both not associated with local wave activity. To account for these effects in part, correlation between peak Hs and peak S_{DF} was determined for wave events at 46013 that exceeded Hs of 2 m, focusing on winter months (Nov.-Mar.) when storm activity is heightened and coastal impacts are greatest, and also the time periods for which analog seismic data have been digitized, 1931-1981.

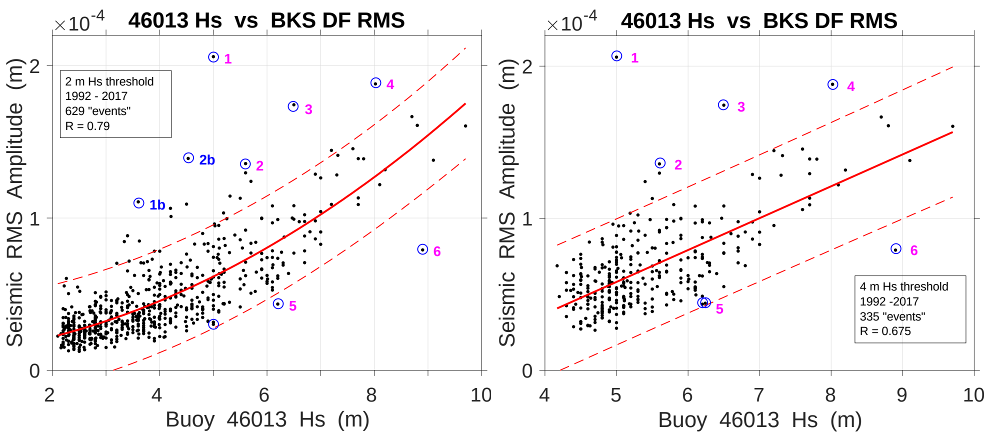

Figure 2. (a) Peak ocean wave Hs vs peak seismic S_{DF} during time periods for wave events that exceed continuously 2 m for at least 6 hr duration, with least squares quadratic trend (solid red) and 95% confidence limits (dashed). (b) Same as (a) except using a 4 m event threshold with a linear fit. Events common to both (a) and (b) (numbered magenta) are outliers, with events 1, 3, 5, and 6 discussed below. (include a location map in Figure 1 along with time series of Hs and DF seismic data ??)

Over the 1992-2017 epoch, 665 events were identified, on average about 6 events per winter month (Figure 2). For each wave event identified, the maximum S_{DF} during the time interval spanning that event was determined. The 2 m Hs threshold during winter was sometimes exceeded continuously for more than two weeks, spanning more than a single wave event. Consequently, for that threshold, some of the S_{DF} peaks do not correspond to particular wave events. However, the relatively large number of events under consideration reduces the impact of these incorrect associations on the underlying statistical relationships, and this typically does not occur for high Hs events.

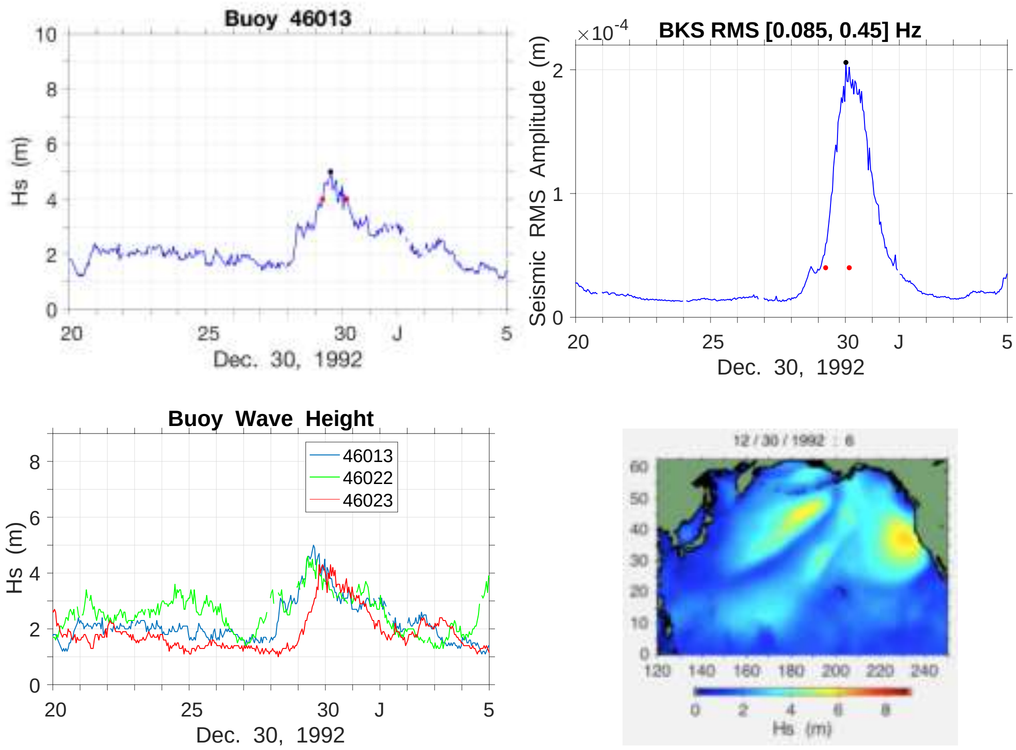

Figure 3. Case 1: Anomalously high DF microseism levels with relatively low Hs. (a) Hs variability at 46013 during the period that includes anomalous event #1 in **Figure 2**, with the 4 m threshold and event duration indicated by red dots, and the event peak (black dot). (b) Same as (a) except for S_{DF} variability at seismic station BKS, with the red dots spanning the same event time in (a). (c) Hs at 46013, northern Humboldt County buoy 46022, and southern Pt. Conception buoy 46023, representing the wave

distribution along most of the California coast. (d) WW3 model Hs over the North Pacific near the Dec. 1992 event peak Hs.

The case of anomalous relatively low Hs at 46013 for observed high microseism levels at BKS is represented by event #1 in **Figure 2**, which is well outside the 95% confidence bound. **Figure 3c** indicates that wave activity is occurring nearly simultaneously along the California coast from the San Francisco region to north of Cape Mendocino, possibly resulting in DF microseism generation along this stretch of coast that is in phase, and thus additively producing the elevated DF levels. Contributions from wave-wave interactions on the continental shelf and/or the deep ocean are possibilities.

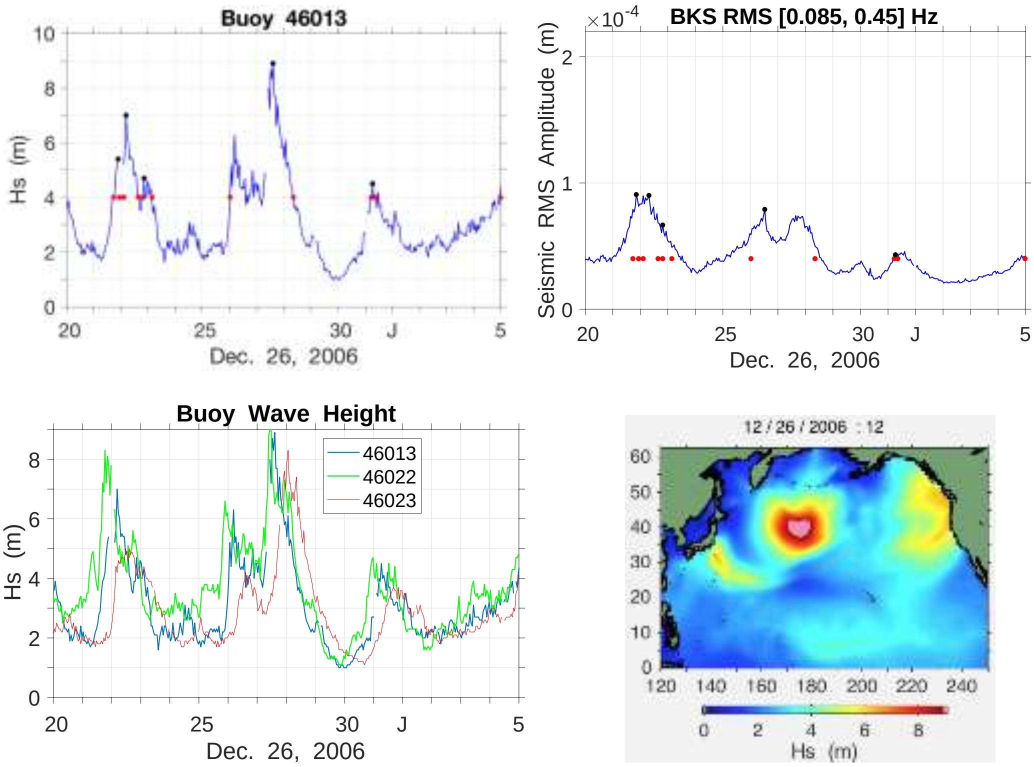

Figure 4. Case 2: Anomalously high Hs with relatively low DF microseism levels. (a)-(d): Same as in **Figure 3** but for anomalous event #6 in **Figure 2** on Dec. 26, 2006.

In contrast to the Dec. 1992 event (**Figure 3**), a representative event the case of an extreme wave Hs event with relatively low seismic DF levels occurred on Dec. 26 (event #6 identified in **Figure 2**). Extreme waves occurred along ghe central and northern California coasts. Differing from event #1, high waves were also observed as far north as the Vancouver B.C. coast. If this wave activity produced in-phase DF generation, then the expectation would be for extreme DF levels as in event #1 in **Figure 2**. However, this did not occur.

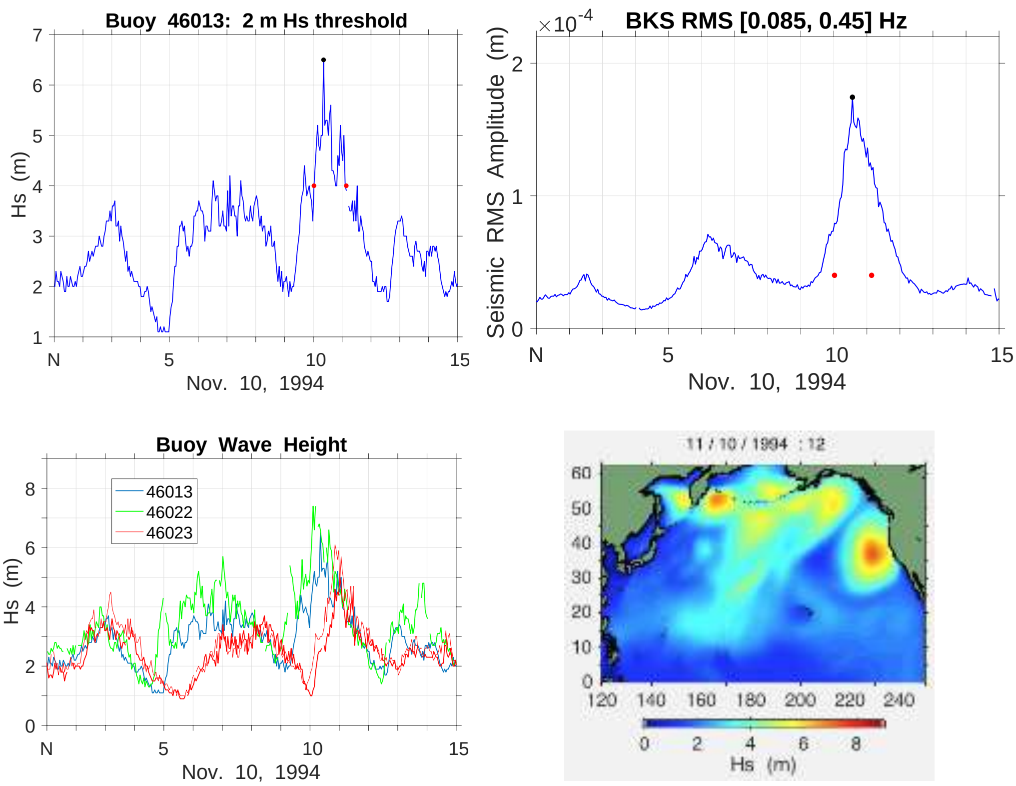

Figure 5. Same as **Figure 3** but for event # 3 in **Figure 2** on Nov. 10, 1994.

The eastern boundary Hs distribution for the Nov. 10, 1994 event (# 3) is similar to that for event # 1 shown in **Figure 3**, but with a somewhat larger extent of somewhat higher Hs. However, the pattern of variability along the California coast is consistent with wave fronts propagating N-S along the coast, in contrast to event #1 in **Figure 3**, suggesting that area of in-phase wave-wave interactions from coastal wave reflections may be smaller for this event, which potentially results in the somewhat lower DF levels observed. **<u>Wave period?</u>**

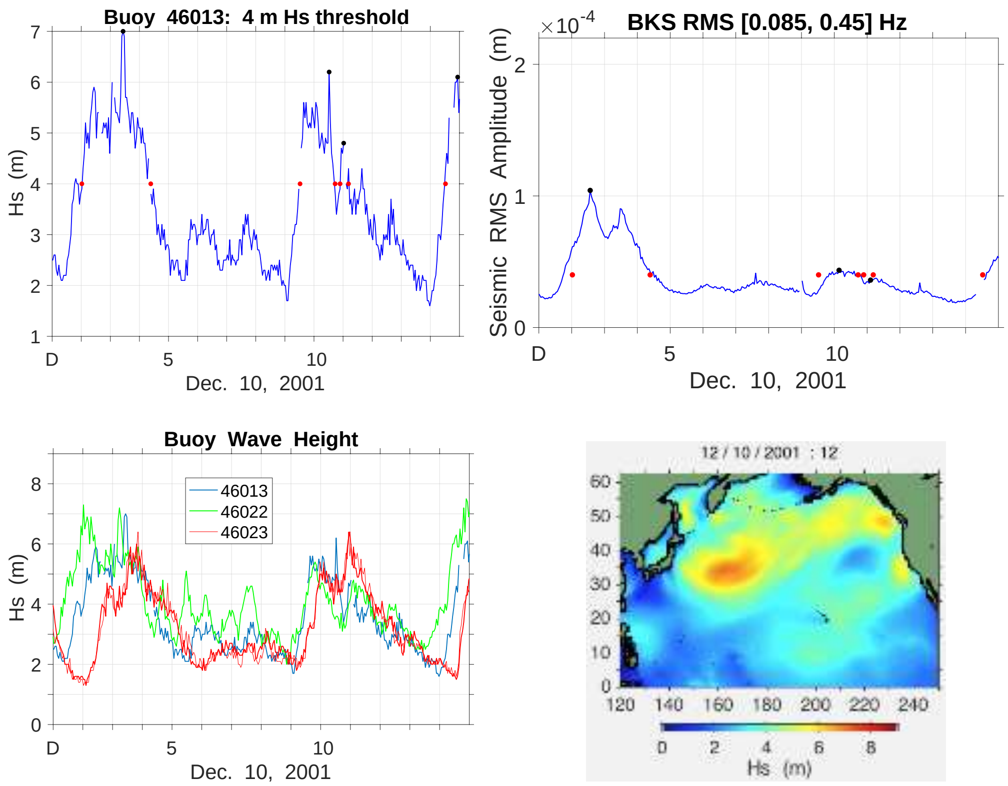

Figure 6. Same as **Figure 3** but for event # 5, i.e. high Hs with low DF levels.

Note that Hs is elevated for for only a short time, suggesting that this Hs peak may be somewhat anomalous in that it potentially results from very local wind activity that will result in wave-wave interactions over a small area and thus not produce high DF levels. Examination of wave spectral energy spectrograms show elevated high frequency components which will not reflect efficiently from the coast, and therefore not provide significant opposing wave components at these higher frequencies to produce elevated DF levels. Also, the wave field itself (**Figure 6d**) has a relatively small areal extent, with waves likely impacting a relatively small coastal region. Note that if the spike for event #5 (**Figure 6a**) was disregarded, it would likely fall within the 95% confidence bounds. Similar short duration Hs spikes may contribute to similar events that appear anomalous.

Seasonal (Nov.-Mar.) Comparison of Buoy Hs and Seismic DF RMS

Realizing that there can be significant differences between 46013 Hs and associated seismic rms levels for particular events, seasonal variability was investigated by determining the mean winter (Nov.-Mar.) levels for all available data for 46013 Hs and BKS rms levels (**Figure 7a**). Their correlation is excellent (R = 0.896), indicating that changes in mean wave activity levels along the central California coast over time can be reliably estimated from changes in DF microseism levels at the Berkeley seismic station.

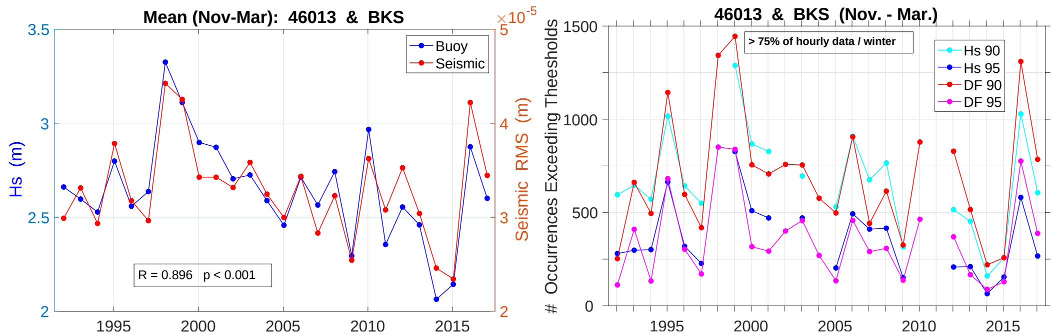

Figure 7. (a) Comparison of mean winter (Nov.-Mar.) 46013 Hs with BKS seismic rms for the [0.085,0.45] Hz band from 1992 to 2017. (b) Number of occurrences of 46013 Hs and BKS DF seismic levels exceeding the 90 and 95 percentile levels determined over the 1992 to 2017 epoch. Winters excluded

either have less than 75% of the total hourly measurements available, which didn't occur for the seismic data, or lack observations that exceed respective thresholds. Thresholds for Hs were 3.5 and 4.0 m, and DF rms of 4.4e-05 and 5.5e-05 m for 90th and 95th percentile thresholds for Hs and DF, respectively.

Comparison of the number of exceedances above selected thresholds between Hs at 46013 and seismic DF levels at BKS shows elevated activity during 1998, 1999, and 2016 winters (**Figure 7b**), consistent with expectations during strong El Ninos, as well as during the exceptional 1995 winter. These show a consistent pattern of variability during winters over the 25 year records.

Later:

Considering all the uncertainties in S_{DF} levels that are poorly constrained, particularly for wave climate reconstruction from the analysis of pre-1980 seismic data, sophisticated methodologies to determine a seismic-to-wave transfer function are likely unwarranted. (maybe in Discussion)